Glucosyloxybenzyl Eucomate Derivatives from Vanda teres Stimulate HaCaT Cytochrome c Oxidase.

ARTICLE *in* JOURNAL OF NATURAL PRODUCTS · MAY 2011

Impact Factor: 3.8 · DOI: 10.1021/np1006636 · Source: PubMed

5 AUTHORS, INCLUDING:

Cyril Antheaume
University of New Caledonia
46 PUBLICATIONS **223** CITATIONS

JOURNAL OF NATURAL PRODUCTS

ARTICLE

pubs.acs.org/jnp

Glucosyloxybenzyl Eucomate Derivatives from *Vanda teres* Stimulate HaCaT Cytochrome *c* Oxidase.

Charlotte Simmler,[†] Cyril Antheaume,[†,§] Patrice André,[‡] Frédéric Bonté,[‡,⊥] and Annelise Lobstein[†]

[†]Faculty of Pharmacy, Strasbourg University, 67400 Illkirch, France

[§]Faculty of Pharmacy, SCA—UMR 7200 67400 Illkirch, France

[⊥]Guerlain, 92290 Levallois Perret, France

[‡]LVMH Recherche, 45800 Saint Jean de Braye, France

Supporting Information

ABSTRACT: Eucomic acid [(2*R*)-2-(*p*-hydroxybenzyl)malic acid)] (**1**) and three new glucopyranosyloxybenzyl eucomate derivatives, vandaterosides I (**2**), II (**3**), and III (**4**), were isolated and identified from the stems of *Vanda teres*. Their cellular antiaging properties were evaluated in a human immortalized keratinocyte cell line (HaCaT) by monitoring their effect on cytochrome *c* oxidase activity, implicated in mitochondrial respiratory function and cellular energy production. Eucomic acid (**1**) and vandateroside II (**3**) increased cytochrome *c* oxidase activity and/or expression, without enhancing cellular mitochondrial content. These two *V. teres* biomarkers apparently contributed to stimulate respiratory functions in keratinocytes. Since aging and its pathologies may be ascribed to a decline in mitochondrial functions, these biomarkers have the potential to become new natural ingredients for antiaging preparations to remedy age-related disorders such as skin aging.

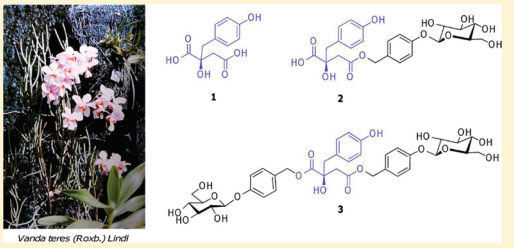

The orchid family is believed to be the second largest family of flowering plants, with almost 30 000 currently registered species, found in 880 genera.[1] However, only a few of them have been investigated regarding their chemical composition and biological activities. Genera from the Epidendroideae subfamily are widely distributed. *Dendrobium*, *Bletilla*, *Cymbidium*, *Gastrodia*, and *Vanda* species occur in tropical areas.[1] The genus *Vanda* comprises 50 to 60 species, mostly found in the southeast of Asia: Thailand, India, Laos, and Burma.[1] Only four *Vanda* species, *V. tessellata* Hook. ex G.Don., *V. parviflora* Lindl., *V. parishii* Rchb.f., and *V. coerulea* Griff. Ex.Lindl, have been chemically investigated, leading to the identification of phenanthropyran derivatives[2,3] and parishin a glucopyranosyloxybenzyl citrate.[4] This last compound and its derivatives were also identified in *Gastrodia elata* Blume tubers.[5] Only *V. tesselata* was tested for its wound-healing properties,[6] whereas phenanthropyrans isolated from *V. coerulea* were analyzed for their antioxidant and anti-inflammatory activities through an inhibition of PGE-2 production on HaCaT.[3] Thus, considering their biological activities on human cells and their chemical composition, Orchidaceae from the genus *Vanda* have not been well studied. These observations led to a focus on *V. teres* (Roxb.) Lindl., also known as *Papilionanthe teres* (Roxb.) Schltr. The isolation, structural elucidation, and first biological investigations of four compounds, namely, eucomic acid (**1**) and three new glycopyranosyloxybenzyl eucomate derivatives, vandaterosides I (**2**), II (**3**), and III (**4**), are herein reported (Scheme 1).

The mitochondrial respiratory chain plays a key role in cell aging processes.[7] Skin epidermal disorders and aging are partly associated with a decline in cellular energy level linked to mitochondrial respiratory chain dysfunctions.[8] Mitochondrial membrane potential is created by electron transfer through respiratory chain enzymatic complexes I—IV. This potential is critical for the proper functioning of this organelle and for ATP production.[7,9] At the end of this respiratory chain, cytochrome *c* oxidase (complex IV) reduces oxygen to form water. Therefore, cytochrome *c* oxidase stimulation could be an appropriate target for any substances that attenuate the cell aging process. Here, the effect of the major constituents of *V. teres* stems, compounds **1** to **4**, on cytochrome *c* oxidase isolated from a human keratinocyte cell line (HaCaT) is reported on.

RESULTS AND DISCUSSION

Isolation and Structural Elucidation of Vandaterosides. The methanolic extract of *V. teres* stems was subjected to Sephadex LH-20 column chromatography eluted successively with H_2O, H_2O/MeOH, and MeOH. Fractions with similar TLC profiles were pooled. Fractions 1, 2, 3, and 5 were subjected to semipreparative RPHPLC to furnish vandaterosides I (0.65%

Received: September 17, 2010
Published: April 21, 2011

Scheme 1. Structures of Eucomic Acid (1) and Vandateroside I (2), II (3), and III (4)

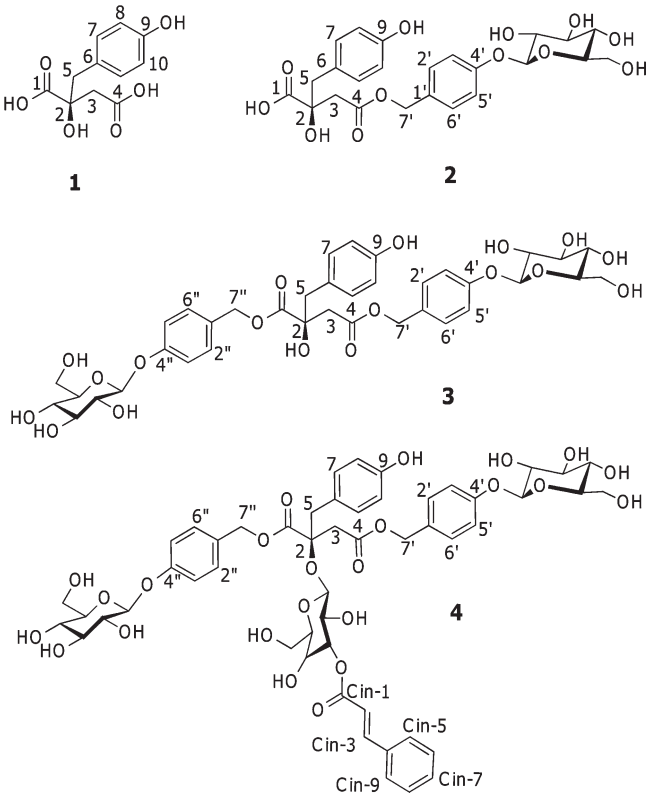

yield, m/m dry material), II (1.33%), and III (0.23%) together with eucomic acid (0.51%).

Vandateroside I (**2**) was obtained as a yellow resin and exhibited a negative specific rotation, $[\alpha]^{20}_{D}$ −50 (*c* 0.1, MeOH). In the UV spectrum, absorption maxima were observed at 203 (log ε 4.08), 225 (log ε 4.04), and 278 nm (log ε 3.16), characteristic of a hydroxybenzyl skeleton. The IR spectrum showed absorption bands at 2512 and 1727 cm^{-1}, corresponding to ester carbonyl and carboxyl functions, and at 1612, 1512, and 1226 cm^{-1}, assignable to an aromatic ring, in addition to strong absorption bands at 3340 and 1074 cm^{-1}, suggestive of a glycoside moiety. Positive HRESIMS revealed a quasi-molecular ion $[(M + NH_4)]^+$ at *m/z* = 526.19236 and revealed the molecular formula of **2** to be $C_{24}H_{28}O_{12}$. The acid hydrolysis of **2** gave D-glucose, which was identified after derivatization by GC-EIMS. The ^1H and ^{13}C NMR ((DMSO-d_6) Table 1) spectra of **2**, which were assigned by 2D gradient NMR experiments (HSQC, HMBC, COSY), showed methoxybenzyl protons [δ 4.98 (2H, s) H_2-7′], two methylene protons [δ 2.41, 2.74 (1H each, both d, *J* = 16.0 Hz) H_2-3; δ 2.77 (2H, m) H_2-5], and two A_2B_2 systems specific to a *para*-substituted aromatic pattern [δ 7.22, 6.98 (2H each, both d, *J* = 8.5 Hz) H-2′/6′, H-5′/3′; δ 6.90, 6.59 (2H each, both d, *J* = 8.5 Hz) H-7/11, H-8/10]. In the HMBC experiment of **2**, H_2-5 correlated with the C-1 (δ_C 171.6) carbonyl carbon and with quaternary carbons C-2 (δ_C 75.3) and aromatic C-6 (δ_C 125.6). The chemically equivalent H-7/11 aromatic protons correlated with the oxygenated C-9 (δ_C 156.0) and with C-5 (δ_C 43.6). In addition H_2-3 gave correlations with C-2, C-1, and C-4 (δ_C 173.7) (Supporting Information). Thus the position of the *para* hydroxybenzyl unit was confirmed, and consequently, C-3 (δ_C 42.4) was located between the two carbonyl functions.

The vandateroside I structure (**2**) shared characteristic features with eucomic acid (**1**) (Scheme 1). The HSQC spectrum clearly showed one glucopyranosyl pattern and one correlation between the anomeric proton (δ 4.84) [(1H, d, *J* = 7.0 Hz), H-4′-*O*-Glc-1] and the anomeric carbon (δ_C 100.5). Furthermore, the aromatic protons H-2′/6′ (δ 7.22) correlated with the aromatic C-4′ (δ_C 157.5) and with C-7′ (δ_C 65.8). The H_2-7′ (δ 4.98) protons correlated with C-4, indicating that the glucosyloxybenzyl moiety was attached to this carbonyl function. Thus, the positions of the β-glucopyranosyl and *p*-hydroxybenzyl alcohol moieties in **2** were defined. On the basis of these findings, the structure of the new compound vandateroside I (**2**) was defined as 4-(4′-β-D-glucopyranosyloxybenzyl)-2-(*p*-hydroxybenzyl)malate, also corresponding to 4-(4′-β-D-glucopyranosyloxybenzyl)-eucomate.

Vandateroside II (**3**) was obtained as a white, amorphous powder and exhibited a negative specific rotation, $[\alpha]^{20}_{D}$ −56 (*c* 0.1, MeOH). In the UV spectrum, absorption maxima were observed at 203 (log ε 4.52), 225 (log ε 4.53), and 278 nm (log ε 3.55), characteristic of a hydroxybenzyl skeleton. The IR spectrum showed absorption bands similar to those of **2**. Positive HRESIMS revealed a quasi-molecular ion $[(M + NH_4)]^+$ at *m/z* = 794.28867, and thus the molecular formula of **3** was calculated for $C_{37}H_{44}O_{18}$. The acid hydrolysis of vandateroside II (**3**) gave D-glucose, which was identified after derivatization by GC-EIMS and comparison with a D-glucose reference. The 1D (^1H, ^{13}C (Table 1)) and 2D NMR spectra of **3** shared common chemical shifts with those of **2**. The ^1H NMR spectrum and HSQC correlations displayed unambiguously a third A_2B_2 system [δ 7.22, 7.00 (2H each, both d, *J* = 8.6 Hz) H-2″/6″, H-5″/3″] linked with a second glucopyranosyl moiety [δ 4.84 (1H, d, *J* = 6.8 Hz) H-4″-*O*-Glc-1], which was confirmed by the HMBC experiment. The HMBC spectrum showed long-range correlations between the following proton and carbon pairs: H-4″-*O*-Glc, H-2″/6″ and C-4″ and between H-2″/6″ and C-7″. The position of the second glucosyloxybenzyl moiety was determined through long-range correlations observed from H_2-7″ (δ 4.96), H_2-3, and H_2-5 to C-1 (δ_C 169.4) (Supporting Information). Thus, the positions of the β-glucopyranosyloxybenzyl and *p*-hydroxybenzyl alcohol moieties in **3** were defined. On the basis of these findings, the structure of vandateroside II (**3**) was defined as 1,4-bis(4′,4″-β-D-glucopyranosyloxybenzyl)-2-(*p*-hydroxybenzyl) malate, also corresponding to 1,4-bis(4′,4″-β-D-glucopyranosyloxybenzyl)eucomate.

Vandateroside III (**4**) was obtained as a yellow resin and exhibited a negative specific rotation, $[\alpha]^{20}_{D}$ −37 (*c* 0.1, MeOH). In the UV spectrum, absorption maxima were observed at 203 (log ε 4.52) and 276 nm (log ε 3.56). The IR spectrum showed absorption bands similar to those of **2** and **3**. The molecular formula of **4**, $C_{52}H_{60}O_{24}$, was determined by the quasi-molecular ion in the positive HRESIMS, $[(M + NH_4)]^+$ at *m/z* = 1086.38484. Its acid hydrolysis liberated D-glucose, which was identified after derivatization by GC-EIMS and comparison with a D-glucose reference. The 1D (Table 1) and 2D NMR spectra showed chemical shifts similar to those of compound **3**. New additional signals corresponding to a third glucopyranosyl moiety [δ 4.82 (1H, d, *J* = 7.8 Hz) H-2-*O*-Glc-1], linked to a *trans*-cinnamate ester [δ 6.67, 7.68 (1H each, both d, *J* = 15.7 Hz), 7.74 (2H, dd, *J* = 2.8, 6.8 Hz), 7.44 (3H, m)], were observed. The

dx.doi.org/10.1021/np1006636 |*J. Nat. Prod.* 2011, 74, 949–955

Table 1. ^{1}H and ^{13}C NMR Spectroscopic Data (400 MHz, 100 MHz, DMSO-d_6) for Vandaterosides I (2), II (3), and III (4)

		vandateroside I (2)		vandateroside II (3)		vandateroside III (4)	
position	mult.	δ_C	δ_H (J in Hz)	δ_C	δ_H (J in Hz)	δ_C	δ_H (J in Hz)
1	C	171.6		169.4		170.0	
2	C	75.3		75.3		80.4	
3a	CH_2	42.4	2.74, d (16.0)	42.3	2.84, d (16.7)	39.5	2.95, d (17.7)
3b			2.41, d (16.0)		2.48, d (16.7)		2.81, d (17.7)
4	C	173.7		173.4		169	
5	CH_2	43.6	2.77, m	43.5	2.81, m	40.8	2.99, m
6	C	125.7		125.4		125.3	
7, 11	CH	131.5	6.90, d (8.5)	131.2	6.91, d (8.5)	131.5	6.96, d (8.5)
8, 10	CH	114.9	6.59, d (8.5)	114.5	6.60, d (8.5)	114.4	6.58, d (8.5)
9	C	156.0		156.0		156.1	
1′	C	129.1		129.0		130.3	
7′	CH_2	65.8	4.98, s	65.1	4.96, s	66.2	5.01, d (6.6)
2′, 6′	CH	129.4	7.22, d (8.5)	129.4	7.25, d (8.6)	129.6	7.26, d (8.6)
5′, 3′	CH	116.2	6.98, d (8.5)	116.0	7.01, d (8.6)	116.2	7.03, d (8.6)
4′	C	157.5		157.1		157.4	
4′-*O*-Glc-1	CH	100.5	4.84, d (7.0)	100.2	4.86, d (6.8)	100.1	4.88, d (7.2)
2	CH	73.1	3.23, m	73.0	3.23, m	73.2	3.23, m
3	CH	77.0	3.35, m	76.8	3.30, m	76.6	3.28, m
4	CH	69.7	3.15, m	69.5	3.15, m	69.7	3.15, m
5	CH	76.6	3.28, m	76.4	3.28, m	77.0	3.33, m
6	CH_2	60.7	3.68, dd (1.5,12.5)	60.5	3.68, dd (4.9,11)	60.7	3.69, dd (1.7,11.7)
			3.45, dd (6.1,12.5)		3.45, dd (5.3,11)		3.45, dd (6.8,11.7)
4″-*O*-Glc-1	CH			100.2	4.84, d (6.8)	100.1	4.87, d (7.2)
2	CH			73.0	3.23, m	73.2	3.23, m
3	CH			76.8	3.30, m	76.6	3.28, m
4	CH			69.5	3.15, m	69.7	3.15, m
5	CH			76.4	3.28, m	77.0	3.33, m
6	CH_2			60.5	3.68, dd (4.9,11)	60.7	3.69, dd (1.7,11.7)
					3.45, dd (5.3,11)		3.45, dd (6.8,11.7)
1″	C			128.9		128.7	
7″a	CH_2			65.6	4.96, s	65.6	4.97, d (5)
7″b							4.93, d (5)
2″, 6″	CH			129.4	7.22, d (8.6)	129.7	7.27, d (8.6)
5″, 3″	CH			115.9	7.00, d (8.6)	116.1	7.03, d (8.6)
4″	C			157.1		157.3	
2-*O*-Glc-1	CH					98.0	4.82, d (7.8)
2	CH					71.6	3.26, m
3	CH					78.0	4.92, t (9.5)
4	CH					67.4	3.39, m
5	CH					76.5	3.10, m
6	CH_2					60.3	3.49, dd (4.5,11.8)
							3.68, dd (1.7,11.8)
Cin-1	C					165.7	
Cin-2	CH					118.4	6.67, d (15.7)
Cin-3	CH					144.2	7.68, d (15.7)
Cin-4	C					134.2	
Cin-5,9	CH					128.3	7.74, dd (2.8, 6.8)
Cin-6,8	CH					128.9	7.44, m
Cin-7	CH					128.7	7.44, m

HMBC spectrum shared similar long-range correlations with the HMBC spectrum of **3**. A long-range correlation was observed between the third anomeric proton H-2-*O*-Glc-1 and C-2 (δ_C 80.4), revealing the position of the third glucosyl unit.

dx.doi.org/10.1021/np1006636 |*J. Nat. Prod.* 2011, 74, 949–955

Long-range correlations were also observed between the proton and carbon pairs of the cinnamyl moiety: H-Cin-6/Cin-8 and C-Cin-4, H-Cin-9 and C-Cin-3, H-Cin-3 and C-Cin-1, and H-Cin-2 and C-Cin-4. In addition, HMBC correlations were observed between H-3 of the 2-*O*-glucosyl unit [δ 4.92 (1H, t, J = 9.5 Hz)] and the anomeric carbon (δ_C 98.0) as well as C-Cin-1 (δ_C 165.7), indicating that the cinnamyl moiety was attached to C-3 of this 2-*O*-glucosyl unit (Supporting Information). Thus, the position of the β-glucopyranosyl-*trans*-cinnamyl ester moiety in **4** was defined. On the basis of these findings, vandateroside III (**4**) was defined as 1,4-bis(4′,4″-β-D-glucopyranosyloxybenzyl)-2-(β-D-glucopyranosyl-3-*trans*-cinnamyl ester)-2-(*p*-hydroxybenzyl)-malate, also corresponding to 1,4-bis(4′,4″-β-D-glucopyranosyloxybenzyl)-2-(β-D-glucopyranosyl-3-*trans*-cinnamyl ester) eucomate.

(2*R*)-2-(*p*-Hydroxybenzyl)malic acid (**1**) was first isolated from the bulbs of *Eucomis punctata* L'Hér. (Liliaceae) and then described as eucomic acid.[10] Eucomic acid (**1**) was also found in *Lycoris radiata* Herb. (Amaryllidaceae), in *Lotus japonicus* (Regel.) K. Larsen (Fabaceae), and in orchid species such as *Cattleya trianaei* Linden & Rchb.f and *Encylica michuacana* Schltr.[11] Eucomic acid, considered as an auxin,[10,11] is consequently not a chemotaxonomic marker of the Orchidaceae family. This auxin shares a common central structure with vandaterosides (Scheme 1) and may be considered as their biosynthetic precursor: vandaterosides could be regarded as glucopyranosyloxybenzyl eucomate derivatives. In addition, the vandateroside glucopyranosyloxybenzyl moiety corresponds to gastrodin, which was first described in *V. parishii*[4] and was also found in *G. elata* tubers.[12] Thus, vandaterosides I (**2**) and II (**3**) can be considered as eucomic acid mono- and digastrodin esters, while vandateroside III (**4**) is a β-3-*trans*-cinnamylglucopyranoside of vandateroside II (**3**).

According to Heller et al.,[10] the absolute configuration of eucomic acid has been determined after comparison with piscidic acid. Eucomic acid displayed a negative specific rotation indicative of 2*R* absolute configuration by comparison with piscidic acid. We observed that our isolated eucomic acid gave a negative specific rotation ($[\alpha]^{20}_D$ −24 in MeOH), in accordance with published data.[10,11] All vandaterosides, considered as eucomic acid mono- and digastrodin esters, displayed negative specific rotation ($[\alpha]^{20}_D$ −50, −56, and −37, in MeOH respectively for vandaterosides I, II, and III). Consequently, after comparison with eucomic acid, the 2*R* absolute configuration of the three vandaterosides was established.

Further phytochemical analyses revealed that vandaterosides I−III were found not only in the stems but also in the leaves and roots of *V. teres*.

Skin aging has been ascribed to mitochondrial dysfunctions and to a subsequent increase of oxidative stress and decline in cellular energy level.[8] Cytochrome *c* oxidase plays a key role in the respiratory chain maintaining mitochondrial membrane potential and participating in cellular energy metabolism.[7,9] On the basis of these premises, it was reasonable to determine whether eucomic acid and vandaterosides I−III could stimulate cytochrome *c* oxidase activity in HaCaT cells.[13]

Stimulation of Cytochrome *c* Oxidase and Mitochondrial Biogenesis. For each concentration tested, vandaterosides I and III did not display any significant stimulation of global cytochrome *c* oxidase activity (Figure 1A). Compared to the control enzyme activity, eucomic acid and vandateroside II showed a significant stimulation of cytochrome *c* oxidase. Eucomic acid (**1**) and vandateroside II (**3**) (at 0.81 μM) activated cytochrome *c* oxidase with 60-fold lower concentrations than resveratrol (at 50 μM) used as the positive control.[14] For all concentrations tested, a tendency for vandateroside II (**3**) to enhance cytochrome *c* oxidase activity (158 ± 33%) more than resveratrol (138 ± 8%) was observed (Figure 1A).

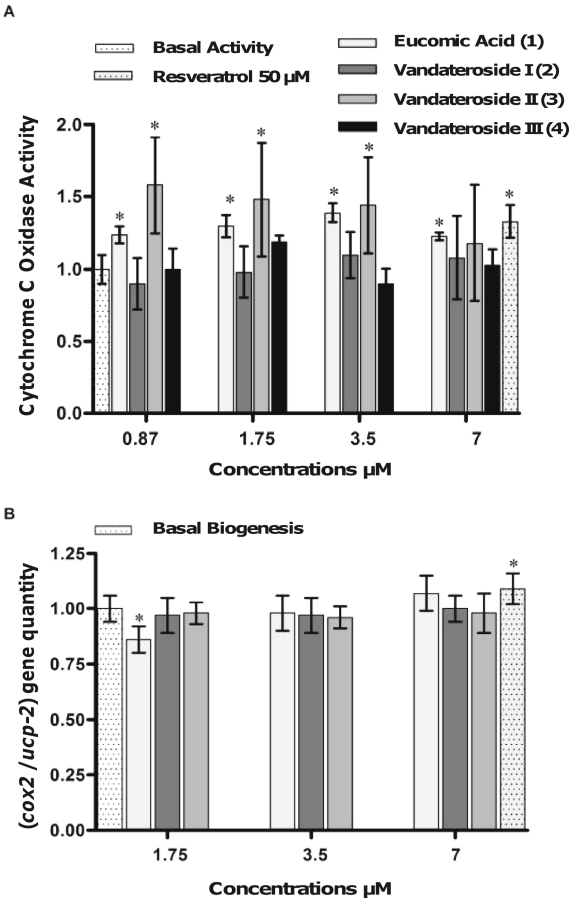

Figure 1. (A) Effects of vandaterosides I−III and eucomic acid on cytochrome *c* oxidase activity. Untreated HaCaT cells were used as negative control and indicated a basal enzyme activity. Cytochrome *c* oxidase activity was expressed as percentage (mean ± SD for three independent experiments) and compared to the basal enzyme activity set at 100 ± 3%. A ratio > 1 indicated a stimulation of cytochrome *c* oxidase. (B) Effects of vandaterosides I and II and eucomic acid on mitochondrial biogenesis. The total quantity of *cox2* mitochondrial gene was compared to the total quantity of *ucp-2* nuclear gene. A ratio *cox2*/*ucp-2* > 1 indicated a stimulation of *cox2* replication, consequently representing mitochondrial biogenesis. Basal mitochondrial biogenesis measured with untreated HaCaT cells was expressed as 100 ± 5% and used as the negative control. Resveratrol (50 μM) was used as the positive control in both experiments. *p < 0.05 compared to the negative control.

An increase in cytochrome *c* oxidase synthesis or in mitochondrial biogenesis could also influence the global stimulation effect measured with eucomic acid and vandateroside II. The mitochondrial biogenesis was evaluated through the quantitation of intracellular mitochondrial DNA. *Cox2* mitochondrial gene encodes expression of cytochrome *c* oxidase subunit II.[15] Thus, whether eucomic acid and vandateroside II could enhance *cox2* quantity and to a lesser extent HaCaT mitochondrial content was examined (Figure 1B). The total quantity of mitochondrial *cox2* gene was compared to the total quantity of *ucp-2* nuclear gene

dx.doi.org/10.1021/np1006636 |*J. Nat. Prod.* 2011, 74, 949–955

encoding the uncoupling protein 2.[16] The negative control was untreated HaCaT cells and reflected a basal *cox2* replication and mitochondrial biogenesis (set at 100 ± 5% for a *cox2/ucp-2* ratio normalized to 1). All results were compared to the negative control. Resveratrol (50 μM) was used as the positive control.[14] Eucomic acid and vandaterosides I and II did not display any increase in *cox2* mitochondrial gene quantity compared to *ucp-2* quantity. Consequently, they did not enhance the HaCaT mitochondrial biogenesis and *cox2* quantity.

The same kind of results were observed with the mitochondrial 16S rRNA gene coding 16S rRNA, a component of the ribosomal protein 30S subunit (data not shown).[15] Consequently, the total level of mitochondria in HaCaT cells was not modified either by eucomic acid (**1**) or by vandaterosides II (**3**) or I (**2**), suggesting that enhancement of cytochrome *c* oxidase activity previously measured was not ascribed to a modification of intracellular *cox2* gene level. Subsequently, vandateroside II (**3**) and eucomic acid (**1**) may increase cytochrome *c* oxidase synthesis or directly stimulate cytochrome *c* oxidase activity.

Interestingly, these glucopyranosyloxybenzyl eucomate derivatives, vandaterosides I–III, are closely related to glucopyranosyloxybenzyl tartrate, malate, and citrate derivatives described in other orchids such as *Coeloglossum viride* (L.) Hartm. var. bracteatum (Willd.),[17] *Gymnadenia conopsea* (L.) R. Br.,[18] and *G. elata*,[5,12] respectively. Dactylorhine B, a glucopyranosyloxybenzyl-2-isobutyl tartrate derivative, was shown to display a stimulating effect on cytochrome *c* oxidase activity and ATP production on rat brain mitochondria.[19] It was demonstrated herein that eucomic acid (**1**) and vandateroside II (**3**) could also stimulate cytochrome *c* oxidase activity and/or expression in the human keratinocyte cell line without enhancing cellular mitochondrial content. Further analyses should be performed to determine whether eucomic acid (**1**) and vandateroside II (**3**) could potentially increase cytochrome *c* oxidase expression.

Deficiencies in cutaneous energy capacity are closely related to alterations in the structure of human skin, especially in the epidermis. Impairment in keratinocyte energy metabolism contributes to a slowdown in skin rejuvenation and wound-healing processes, leading to a thinner epidermis with a reduced protective function.[8] Our results reveal that eucomic acid and vandateroside II stimulate cellular respiratory functions through cytochrome *c* oxidase and consequently have the potential to fight signs of epidermal aging.

EXPERIMENTAL SECTION

General Experimental Procedures. The following instruments were used to obtain physical data: optical rotations, Perkin-Elmer 341 polarimeter (l = 1 cm); UV spectra, Shimadzu UV-2401PC spectrometer; IR spectra, Nicolet 380 FT-IR (Thermo Electron Corporation); ^{1}H and ^{13}C NMR spectra, Bruker (400 MHz-100 MHz) Avance III spectrometer with TMS as internal standard; all the chemical shifts (δ) were reported in parts per million (ppm) relative to TMS (δ = 0); ESIMS and HRESIMS, HPLC Agilent 1200RRLC equipped with an Agilent 6520 Accurate Mass QTOF spectrometer; GC-MS and EIMS, Trace GS Ultra equipped with a capillary TR-5MS SQC column (0.25 μm, 15 m × 0.25 mm i.d.) and DSQII Thermo Scientific mass spectrometer; HPLC detector, Prostar 330 diode-array detector and UV–vis 151 Gilson wavelength detector; HPLC column, Nucleodur C18ec column (5 μm, 250 mm × 4.6 mm i.d.) and Nucleodur C18ec column (5 μm, 250 mm × 21 mm i.d.) used for analytical (flow rate 1 mL·min^{-1}) and semipreparative (14 mL·min^{-1}) profiles, respectively. The column was eluted with MeOH/(H_2O + 0.1% HCO_2H) using a linear gradient starting from 20% up to 47% MeOH in 13.5 min, maintaining 47% MeOH during 10 min, and finally from 47% to 100% MeOH in 10 min. The fractions were monitored between 200 and 400 nm.

Reagents for Biological Analyses. Resveratrol, DMSO, all other chemicals, cytochrome *c* (from equine heart), Bradford solution, and bovine serum albumin (BSA) were obtained from Sigma (Lyon, France). Cell proliferation kit II reagent (XTT) was provided by Roche Diagnostic (Meylan, France). Bicinchoninic acid (BCA) assay kit for protein dosage was obtained from Uptima Interchim (Montluçon, France). Dulbecco's minimum essential medium (DMEM), fetal bovine serum (FBS) for HaCaT culture, penicillin/streptomycin, and glutamine were purchased from Invitrogen (Cergy-Pontoise, France), and MIX-PCR SYBR Green was obtained from Applied Biosystems (Courtaboeuf, France).

Plant Material. *Vanda teres* was identified by Dr. Josef Margraf in Thailand. A voucher specimen (No P-th-1004) was deposited at the quarantine office of the Bangkok Agricultural Department. Stems from flowering specimens were collected in October 2006.

Cut stems were dried in the sunshine in hanging baskets, so as to avoid contamination by soil and to prevent fungus development. After arrival in France, dried, cut stems were pulverized in an ultracentrifuge crusher (Retsch ZM 200) just before extraction. The collection of stems was carried out in accordance with CITES (Convention on International Trade in Endangered Species of Wild Fauna and Flora) regulations.

Extraction and Isolation. Dried *V. teres* stems (100 g) were successively extracted by cyclohexane, CH_2Cl_2, and MeOH using an automatic Soxhlet (Avanti 2055) to yield cyclohexane (1.8 g), CH_2Cl_2 (1.4 g), and MeOH (6.9 g) extracts, respectively. An aliquot of the MeOH extract (1 g) was suspended in H_2O/MeOH (95:5) and subjected to a Sephadex LH-20 column (30 g) with a H_2O/MeOH elution gradient (from 100% H_2O to 100% MeOH) to yield 20 fractions of 10 mL each. Fractions with similar TLC profiles were pooled to give eight fractions. Fractions 1 (424 mg), 2 (178 mg), 3 (65 mg), and 5 (40 mg) were further purified by semipreparative RPHPLC with the same gradient elution, a flow rate of 14 mL·min^{-1}, and detection at 205 nm. Compound **1** (60 mg) was obtained from fractions 1 and 2, and compounds **2** (68 mg), **3** (125 mg), and **4** (20 mg) were obtained from fractions 2, 3, and 5, respectively. Compound **1** was identified as (2*R*)-2-(hydroxybenzyl)malic acid, also known as eucomic acid, by physical data comparison ($[\alpha]_D$, UV, ^{1}H and ^{13}C NMR, MS) with reported data.[10,11]

Acid Hydrolysis of Compounds 2–4. A solution of **2**–**4** (each 2 mg) in 2 M HCl (0.5 mL) was heated under reflux for 3 h. After cooling, the solution was extracted with *n*-BuOH. The dried residue of the aqueous layer was derivatized by pyridine and 1-(trimethylsilyl)-imidazole (4:1 v/v) during 1 h at 60 °C. The mixture was analyzed by GC-MS (Trace GS Ultra) with a capillary TR-5MS SQC column (0.25 μm, 15 m × 0.25 mm) under the following conditions: 1 min at 40 °C, increase of temperature with a thermal ramp of 10 °C/min until 250 °C (helium flow rate 1 mL·min^{-1}, injector temperature 250 °C, transfer temperature 285 °C). Impact electronic detection was carried out with a DSQII Thermo Scientific mass spectrometer, mass detection ranges from 0 to 500. Identification of D-glucose was performed by comparison of its retention time and spectroscopic data with those of an authentic sample of D-glucose (Merck K3398837), t_R 15.6 min.

Eucomic acid (1): white needles (MeOH), $[\alpha]^{20}_D$ −24 (c 0.1, MeOH); UV (in MeOH) λ_{max} (log ε) 203 (3.9), 224 (3.9), and 278 (3.2) nm; ^{1}H NMR (MeOH-d_4, 400 MHz) δ 4.00 (1H, d, J = 16 Hz, H-3a), 4.33 (1H, d, J = 16 Hz, H-3b), 4.29 (1H, d, J = 13.7 Hz, H-5a), 4.38 (1H, d, J = 13.7 Hz, H-5b), 8.50 (2H, d, J = 8.5 Hz, H-7/11), 8.11 (2H, d, J = 8.5 Hz, H-8/10); ^{13}C NMR (MeOH-d_4, 100 MHz) δ 174.9 (C-1), 77.0 (C-2), 44.1 (C-3), 178.3 (C-4), 45.5 (C-5), 127.9 (C-6), 132.8 (C-7 and C-11), 115.9 (C-8 and C-10), 157.5 (C-9); HRESIMS m/z 239.05549 (calcd for $C_{11}H_{11}O_6$, 239.05611, Δ 2.6 ppm).

dx.doi.org/10.1021/np1006636 |J. Nat. Prod. 2011, 74, 949–955

Vandateroside I (2): yellowish resin, $[\alpha]^{20}_{D}$ −50 (*c* 0.1, MeOH); UV (in MeOH) λ_{max} (log ε) 203 (4.08), 225 (4.04), and 278 (3.16) nm; ν_{max} 3340.2, 2512, 1727, 1612, 1512, 1226 and 1042, 1074 cm^{-1}; ^1H and ^{13}C NMR data (DMSO-d_6, 400 MHz) see Table 1; HRESIMS *m/z* 526.19236 (calcd for $C_{24}H_{32}NO_{12}$, 526.19190, Δ = −0.87 ppm).

Vandateroside II (3): white, amorphous solid, $[\alpha]^{20}_{D}$ −56 (*c* 0.1, MeOH); UV (in MeOH) λ_{max} (log ε) 203 (4.52), 225 (4.53), and 278 (3.55) nm; ν_{max} 3340.2, 2512, 1727, 1612, 1512, 1074 and 1068, 1014 cm^{-1}; ^1H and ^{13}C NMR data (DMSO-d_6, 400 MHz) see Table 1; HRESIMS *m/z* 794.28867 (calcd for $C_{37}H_{48}NO_{18}$, 794.28659, Δ = −2.66 ppm).

Vandateroside III (4): yellowish resin, $[\alpha]^{20}_{D}$ −37 (*c* 0.1 MeOH); UV (in MeOH) λ_{max} (log ε) 203 (4.52), and 276 (3.56) nm; ν_{max} 3340.2, 2359, 23411727, 1612, 1512, 1074 and 1068, 1014 cm^{-1}; ^1H and ^{13}C NMR data (DMSO-d_6, 400 MHz) see Table 1; HRESIMS *m/z* 1086.38484 (calcd for $C_{52}H_{64}NO_{24}$, 1086.38128, Δ = −3.28 ppm).

Activation of Mitochondrial Cytochrome *c* Oxidase in HaCaT Cells. HaCaT cells (90% confluent, provided by LVMH Recherche) cultured in six-well plates were treated for 3 h in DMEM (4.5 g/L glucose) with 0.1% BSA with serial dilutions of compounds **1**−**4** in DMSO (0.1% v/v final concentration). Resveratrol at 50 μM was used as the positive control.[14] HaCaT cells were lysed in a HEPES buffer (20 mM HEPES, 0.1%Triton, 1 mM EDTA). Total proteins were quantified using a Bradford solution, and samples were adjusted to 2 $mg \cdot mL^{-1}$. Each cell lysate was first incubated with the assay buffer (Sigma) to determine the v^0 (speed of enzyme without added substrate); 50 μM reduced cytochrome *c* (from equine heart) was added to determine the speed of the enzymatic reaction. The disappearance of reduced cytochrome *c* was followed with a spectrophotometer at 550 nm during 90 s (according to the manufacturer's instructions, Sigma). The results were calculated from the slopes and expressed as activity of cytochrome *c* oxidase (U/μg). The enzymatic activities measured with vandaterosides (A_{COX} sample) were compared to the negative control (basal cytochrome *c* oxidase activity: A_{COX} control DMSO 0.1%). Stimulation of cytochrome *c* oxidase was determined with a ratio A_{COX} sample/A_{COX} control > 1.

Mitochondrial Biogenesis Measurement. HaCaT cells were cultivated and treated as described previously. After 48 h treatment, total cell lysates were obtained using a lysis buffer (Tris-base 10 mM, EDTA 1 mM, NaOAc 0.3 M, SDS 1%). DNA was extracted from cell lysates with a phenol solution (1:1) and centrifuged two times at 4000 rpm during 5 min. In the supernatant containing DNA, a solution of $CHCl_3$/isoamyl alcohol (24:1 v/v) was added. Precipitation of total DNA was done with absolute EtOH/3 M NaOAc (2.5:1/10 v/v). DNA quantification was performed with a Nanodrop spectrometer (Thermo Scientific), and solutions were adjusted to a final concentration of 10 $ng \cdot \mu L^{-1}$. Three kinds of genes were quantified by qPCR: mitochondrial genes 16S rRNA and *cox2*[15] and nuclear gene *ucp-2*[16] used as internal control. PCR primers are listed below: DNA 16S rRNA: sense strand (5′-TGGACAACCAGCTATCACCA-3′), antisense strand (5′-ACTTTGCAAGGAGAGCCAAA-3′); DNA *cox2*: sense strand (5′-AGGCGACCTGCGACTCCTTGA-3′) and antisense strand (5′-TTAGCTTTACAGTGGGCTCTAGAGGC-3′); DNA *ucp-2*: sense strand (5′-CCTAGCGCTGCCTCATAAAC-3′) and antisense strand (5′-CCTATGGGTCTGTGCCTGTT-3′). Total cell DNA samples were mixed with MIX-PCR SYBR Green and deionized H_2O. Fluorescence was read after 45 PCR cycles at 60 °C. Serial dilutions of a total DNA solution were prepared for each primer to obtain a calibration curve. Results were expressed as quantity of 16S rRNA (Q_{16S}) and *cox2* (Q_{COX}) DNA compared to nuclear *ucp-2* DNA (Q_{UCP-2}). Results were compared with the negative control (untreated HaCaT cells). An increase in *cox2* gene quantity and thus in mitochondrial biogenesis was considered with a ratio $(Q_{COX})/(Q_{UCP-2})$ > 1 compared with the negative control. Resveratrol was used as the positive control.[14]

Cytotoxicity Assay. Cell viability was previously evaluated by XTT analysis as described by Roehm et al.,[20] and results were interpreted after comparison of total cell protein measurement by a BCA assay. Serial dilutions of **1**−**3** were prepared in DMSO (0.1% v/v final concentration). The first higher concentration tested on HaCaT cells was not cytotoxic (data not shown).

Statistical Analyses. In vitro experiments were performed three times. All data were expressed as means ± standard deviations. Comparison of results was performed by Student's paired *t* test analysis. Statistical significance was set at $p < 0.05$.

■ ASSOCIATED CONTENT

Supporting Information. HPLC profile of *V. teres* stem crude extract, ^1H and ^{13}C NMR spectra of vandaterosides I, II, and III, and key HMBC correlations are available free of charge via the Internet at http://pubs.acs.org.

■ AUTHOR INFORMATION

Corresponding Author
Tel: +033 368 8542 41. Fax: +033 368 8543 10. E-mail: charlotte.simmler@pharma.u-strasbg.fr.

■ ACKNOWLEDGMENT

Dr. R. Saladin and Dr. J. Brent Friesen are gratefully acknowledged for helpful comments during the preparation of the manuscript.

■ REFERENCES

(1) (a) Lecoufle, M. *Le Traité des Orchidées*; Artémis Edition: Losange, 2004; p 42. (b) Chase, M. W., Cameron, M. K., Barret, R. L., Freudenstein, J. V. *DNA Data and Orchidaceae Systematic: a New Phylogenetic Classification* URL, http://www.orchids.co.in/dna-data-orchidaceae-shtm. 2005, accessed Aug 9, 2010.

(2) (a) Anuradha, V.; Prakasa Rao, N. S. *Phytochemistry* **1998**, *48*, 183–184. (b) Anuradha, V.; Prakasa Rao, N. S. *Phytochemistry* **1998**, *48*, 181–182.

(3) Simmler, C.; Antheaume, C.; Lobstein, A. *Plosone* **2010**, *5*, e13713.

(4) Dahmen, J.; Leander, K. *Phytochemistry* **1976**, *15*, 1986–1987.

(5) (a) Li, J. H.; Liu, Y. C.; Hau, J. P.; Wen, K. C. *Phytochemistry* **2002**, *42*, 549–551. (b) Li, N.; Wang, K. J.; Chen, J. J.; Zhou, J. *J. Asian Nat. Prod. Res.* **2007**, *42*, 373–377.

(6) Nayak, B. S.; Suresh, R.; Rao, A. V.; Pillai, G. K.; Davis, E. M.; Ramkissoon, V.; McRae, A. *Int. J. Low. Extrem. Wounds* **2005**, *4*, 200–204.

(7) (a) Lanza, I. R.; Nair, K. S. *Pflugers Arch.* **2010**, *459*, 277–289. (b) Bratica, I.; Trifunović, A. *Biochim. Biophys. Acta* **2010**, *1797*, 961–967.

(8) (a) Menon, G. K.; Dal Farra, C.; Botto, J. M.; Domloge, N. *J. Cosmet. Dermatol.* **2010**, *9*, 122–131. (b) Blatt, T.; Lenz, H.; Koop, U.; Jaspers, S.; Weber, T.; Mummer, C.; Wittern, K. P.; Stäb, F.; Wenck, H. *Biofactors* **2005**, *25*, 179–185.

(9) Capaldi, R. A. *Annu. Rev. Biochem.* **1990**, *59*, 569–596.

(10) Heller, W.; Tamm, C. *Helv. Chim. Acta* **1974**, *57*, 1766–1784.

(11) (a) Koizumi, T.; Isogai, Y.; Nomoto, S.; Okamoto, T. *Phytochemistry* **1976**, *15*, 342–343. (b) Minoru, I.; Shunpei, U.; Kunimitsu, F.; Mizuo, N.; Yukihiro, S.; Yumi, M.; Itsuo, N. *Phytochemistry* **1979**, *18* 1211–1213. (c) Tovar-Gijón, C. E.; Hernández-Carlos, B.; Burgueño-Tapia, E.; Cedillo-Portugal, E.; Joseph-Nathan, P. *J. Mol. Struct.* **2006**, *783*, 96–100. (d) Okada, M.; Park, S.; Koshizawa, T.; Ueda, M. *Tetrahedron* **2009**, *65*, 2136–2141.

(12) (a) Liu, C. L.; Liu, M. C.; Zhu, R. L. *Chromatographia* **2002**, *55*, 317–320. (b) Yang, X. D.; Zhu, J.; Yang, R.; Liu, J. P.; Li, L.; Zhang, H. B. *Nat. Prod. Res.* **2007**, *21*, 180–186.

(13) (a) Savignan, F.; Ballion, B.; Odessa, M. F.; Charveron, M.; Bordat, P.; Dufy, B. *J. Biomed. Sci.* **2004**, *11*, 671–682. (b) Paz, M. L.; González Maglio, D. H.; Weill, F. S.; Bustamante, J.; Leoni, J. *Photodermatol. Photoimmunol. Photomed.* **2008**, *24*, 115–122.

(14) (a) Csiszar, A.; Labinskyy, N.; Pinto, J. T.; Ballabh, P.; Zhang, H.; Losonczy, G.; Pearson, K.; de Cabo, R.; Pacher, P.; Zhang, C.; Ungvari, Z. *Am. J. Physiol. Heart Circ. Physiol.* **2009**, *297*, H13–H20. (b) López-Lluch, G.; Irusta, P. M.; Navas, P.; de Cabo, R. *Exp. Gerontol.* **2008**, *43*, 813–819.

(15) Anderson, S.; Bankier, A. T.; Barrell, B. G.; de Bruijn, M. H.; Coulson, A. R.; Drouin, J.; Eperon, I. C.; Nierlich, D. P.; Roe, B. A.; Sanger, F.; Schreier, P. H.; Smith, A. J.; Staden, R.; Young, I. G. *Nature* **1981**, *290*, 457–465.

(16) (a) Wolkow, C. A.; Iser, W. B. *Ageing Res. Rev.* **2006**, *5*, 196–208. (b) Ricquier, D.; Bouillaud, F. *Biochem. J.* **2000**, *345*, 161–179.

(17) (a) Huang, S. Y.; Shi, J. G.; Yang, Y. C.; Tu, P. F. *Chin. Chem. Lett.* **2003**, *14*, 814–817. (b) Huang, S. Y.; Li, G. Q.; Shi, J. G.; Mo, S. Y. *J. Asian Nat. Prod. Res.* **2004**, *6*, 59–61. (c) Li, M.; Guo, S. X.; Wang, C. L.; Xiao, P. G. *J. Chromatogr. Sci.* **2009**, *47*, 709–713.

(18) (a) Morikawa, T.; Xie, H.; Matsuda, H.; Yoshikawa, M. *J. Nat. Prod.* **2006**, *69*, 881–886. (b) Morikawa, T.; Xie, H.; Matsuda, H.; Wang, T.; Yoshikawa, M. *Chem. Pharm. Bull.* **2006**, *54*, 506–513. (c) Zi, J.; Li, S.; Liu, M.; Gan, M.; Lin, S.; Song, W.; Zhang, Y.; Fan, X.; Yang, Y.; Zhang, J.; Shi, J.; Di, D. *J. Nat. Prod.* **2008**, *71*, 799–805.

(19) Zhang, D.; Zhang, Y.; Liu, G.; Zhang, J. *Naunyn Schmiedebergs Arch. Pharmacol.* **2006**, *374*, 117–125.

(20) Roehm, N. W.; Rodgers, G. H.; Hatfield, S. M.; Glasebrook, A. L. *J. Immunol. Methods* **1991**, *142*, 257–265.